Polym. Bull. (2015) 72:3097–3117
DOI 10.1007/s00289-015-1455-8

ORIGINAL PAPER

Synthesis of amphiphilic alginate derivatives and electrospinning blend nanofibers: a novel hydrophobic drug carrier

Xiuqiong Chen[1] · Huiqiong Yan[1] · Wei Sun[1] · Yuhong Feng[2] · Jiacheng Li[2] · Qiang Lin[1] · Zaifeng Shi[1] · Xianghui Wang[1]

Received: 10 January 2015 / Revised: 12 June 2015 / Accepted: 5 July 2015 /
Published online: 5 August 2015

Abstract As a kind of novel hydrophobic drug carrier materials, the drug-loaded nanofibers were successfully fabricated using amphiphilic alginate derivative (AAD) and poly (vinyl alcohol) (PVA) by electrospinning method. The AAD was synthesized by amide linkage attachment of octylamine onto the carboxylic group of alginate, which was characterized by the means of elemental analysis, FT-IR spectrometer, ^{1}H NMR spectrometer and fluorescence measurement. Experimental results showed the amidation of alginate was successful, in which the degree of modification was 0.27 and the critical aggregation concentration in 0.15 mol/L aqueous NaCl solution was 0.43 mg/mL. The octyl groups of AAD could effectively make alginate chains flexible and enhance chain entanglements through the hydrophobic interactions between octyl groups. In contrast to sodium alginate (SA)/PVA blend solutions, AAD/PVA blend solutions showed more excellent electrospinnability. Additionally, the different volume ratios of SA or AAD to PVA played an important role in the formation and morphology of the electrospun blend nanofibers. Although the amidation of alginate could not fundamentally alter the spinnability of alginate, the content of alginate in the blend nanofibers was appropriately increased. The new generated drug-loaded AAD/PVA (20/80) blend nanofibers exhibited relatively continuous and uniform nanofibers with the average diameter of 191.72 nm. Compared to the drug-loaded SA/PVA (20/80) blend

✉ Jiacheng Li
ljcfyh@gmail.com

✉ Qiang Lin
linqianggroup@163.com; linqiang1962@gmail.com

[1] College of Chemistry and Chemical Engineering, Hainan Normal University, Haikou 571100, Hainan, People's Republic of China

[2] Key Laboratory of Ministry of Education for Application Technology of Chemical Materials in Hainan Superior Resources, College of Materials and Chemical Engineering, Hainan University, Haikou 570228, People's Republic of China

nanofibers, the drug-loaded AAD/PVA (20/80) blend nanofibers presented a sustained release performance with the slow release of about 76 % λ-cyhalothrin during the initial period of 10 h.

Keywords Alginate · Amphiphilic alginate derivative · The amidation · Poly (vinyl alcohol) · Electrospinning · Blend nanofibers

Introduction

Electrospinning is a straightforward method of generating ultrafine fibers on a nanoscopic scale with controlled surface morphology [1]. Due to their high specific surface area and porous structure [2], the electrospun nonwoven fabrics that consisted of ultrafine fibers have found wide biomedical applications such as scaffolds for tissue engineering [3, 4], wound dressing materials [5] and carriers for drug delivery [6]. Many polymers have been successfully electrospun as promising materials for several years [7–10]. Especially, alginate, as a biopolymer for preparing nanofibers, has attracted a lot of attention in recent years [11].

Alginate is a linear anionic polysaccharide consisted of 1, 4-β-D-mannuronic acid (M block) and C-5 epimer α-L-guluronic acid (G block) units with different proportions of arrangements in GG, MG and MM blocks [12, 13]. It has been regarded as an excellent polysaccharide for drug delivery system due to its good properties such as nontoxicity, immunogenicity, biocompatibility and biodegradability [14–17]. However, pure alginate has its inherent drawbacks such as poor mechanical strength, uncontrolled degradation and extensive water uptake properties [18, 19], which restrict its real applications [20]. It has been reported that amphiphilic alginate derivative modified by introducing the hydrophobic groups into the hydrophilic polysaccharide is not only a good candidate for the formation of nanoparticles, but also an effective way to enhance its affinity to the hydrophobic drug [21–23]. However, pure alginate can hardly be electrospun into nanofibers, and the electrospinnability of pure alginate could be improved by introducing a strong polar cosolvent, glycerol [24], introducing Ca^{2+} cations [11] or adding small amount of surfactants [25] into its aqueous solution. The successfully electrospun alginate fibers are all based on the blend solutions of alginate and poly (ethylene oxide) (PEO) or alginate and poly (vinyl alcohol) (PVA) [26–28].

It has been reported that the rigidity of the alginate chain is mainly caused by its intramolecular hydrogen bonding formed by –COOH and –OH, which hinders the formation of effective chain entanglements in its aqueous solution [29, 30]. For this reason, electrospinning of pure alginate from its aqueous solution is difficult to be achieved. Therefore, the purpose of our study is to test whether the electrospinnability of alginate solution could be improved by reducing its intramolecular hydrogen bonding. The amidation of alginate is easily carried using the coupling agent 1-ethyl-3-(3-dimethyl-aminopropyl) carbodiimide hydrochloride (EDC·HCl) to form amide linkages between octylamine molecules and the carboxylic moieties on the alginate polymer backbone [23]. This process could destroy the original intramolecular hydrogen bonding of alginate and reduce the chain rigidity, thus

improving the flexibility of the molecular chain. Therefore, it can be assumed that the amidation of alginate would improve the fabrication of nanofibers. To our knowledge, the improvement of alginate's electrospinnability by the amidation has not been reported previously. Additionally, the physical properties of alginate solution, such as surface tension and conductivity, have great effects on the electrospinnability of alginate solution. Bonino et al. reported the usage of PEO as carrier materials to prepare alginate nanofibers, and found that surface tension of the solutions had the greatest effect on whether the blend solutions could be electrospun [25]. Nie et al. found that the blend solutions of glycerol and alginate could be electrospun and this strong polar cosolvent could decrease surface tension and conductivity of alginate solution [24].

In this study, the octyl-grafted amphiphilic alginate derivative (AAD) was prepared by amide linkage attachment of octyl amine onto the carboxylic group of alginate. λ-Cyhalothrin, a kind of pyrethroid insecticide widely used in controlling insect pests in agriculture, was selected as the model pesticide as it is the representative of hydrophobic organic pesticides [31]. To improve the physical properties of SA/PVA blend solutions, PVA was used due to its good properties such as fiber forming ability, good flexibility, biocompatibility, chemical resistance and biodegradability [15, 32]. The mixture of AAD aqueous solution and PVA aqueous solution was electrospun to investigate whether the octyl-grafted AAD could improve the electrospinnability of alginate solution. The release behaviors of λ-cyhalothrin from its electrospun fibers under 50 % methanol aqueous medium were studied by comparing the release behaviors of the pesticides from AAD/PVA blend nanofibers and SA/PVA blend nanofibers. This study examined the influences of AAD on improving the electrospinnability of SA solution and the solution physical properties, surface tension and conductivity on the electrospinnability and fiber morphology. Further studies on rheology, thermal properties of AAD/PVA blend nanofibers will be investigated in our next work. This study aimed at combining the affinity to the hydrophobic drug and improved electrospinnability of amphiphilic alginate derivative to develop a novel hydrophobic drug carrier.

Experimental sections

Materials

Sodium alginate (SA, $M_W = 432$kda), octylamine, poly (vinyl alcohol) (PVA, $M_n = 1750$), 1-ethyl-3-(3-dimethyl-aminopropyl) carbodiimide hydrochloride (EDC·HCl), HCl, ethanol, methanol, NaCl and pyrene were purchased from Aladdin Chemical Reagent Co., Ltd., Shanghai, China. The chemicals were of analytical grade and used without further purification. λ-Cyhalothrin (>94.6 %) was provided by Yangnong Reagent Co., Ltd., Chemical, Jiangsu, China. Distilled water was used as a solvent to prepare all solutions.

Methods

Synthesis and characterization of AAD

Amphiphilic alginate derivative (AAD) was synthesized by the amidation through alginate coupling with octylamine in the presence of EDC·HCl [23, 33–35]. The amidation reaction was carried out through the following steps. First, 5.00 g of SA was dissolved in a volume of 200 mL of distilled water and the pH value of the solution was adjusted to 3.4 by 0.5 mol/L HCl. Then, 3.40 g of EDC·HCl was added to the solution with the pH value of the mixture maintained at 3.4 by the addition of 0.5 mol/L HCl. Subsequently, the alginate solution was diluted to a concentration of 2.0 wt% and reacted for 10 min, then 6.0 mL of octylamine was added and the mixture was stirred at 35 °C for 24 h. Finally, 1000 mL of ethanol was added to precipitate the product, which was centrifuged, washed with ethanol and dried at 40 °C to obtain the product. The product was dialyzed in distilled water for 3 days and lyophilized for 2 days to get the pure AAD product.

The degree of amidation of SA was calculated based on the N/C ratio and determined by a Vario EL cube elemental analyser (Elementar-Germany). The structure of AAD was confirmed by FT-IR and ^{1}H NMR. FT-IR spectra of sample were recorded on a Tensor 27 Fourier transform infrared spectrometer (Bruker, Germany). The samples were mixed with KBr and compressed to semitransparent disks for spectroscopic analysis. ^{1}H NMR was performed on an AV 400 nuclear magnetic resonance spectrometer (Bruker, Germany). The samples were dissolved in D_2O to the concentration of 10 mg/mL. The critical aggregation concentration of AAD in 0.15 mol/L aqueous NaCl solution was determined by fluorescence measurement [36] using a F7000 fluorescence spectrophotometer (Hitachi, Japan). Pyrene as a fluorescence probe was excited at 335 nm and the emission spectrum was collected in the range of 335–600 nm at an integration time of 1 s with the slit width of 2.5 nm.

Fabrication of AAD/PVA blend nanofibers and drug-loaded AAD/PVA blend nanofibers

2.0 wt% AAD solution and 10.0 wt% PVA solution were prepared by dissolving precise amount of reagents in distilled water and continuously stirred at 60 °C for 3 h and 80 °C for 5 h, respectively. Then, AAD solution was mixed with PVA solution to obtain the blend solutions with various volume ratios of AAD to PVA ranging from 70/30 to 20/80. After the blend solutions were left for 30 min to eliminate any air bubbles, electrospun nanofibers were achieved via a syringe using a high voltage power (Machinery & Electricity Institute Co., Ltd., Beijing, China) with the applied voltage adjusted to 10–20 kV. Moreover, a flow rate of 0.4 mL/h, a temperature of 25 °C and humidity of 40 % were used. Fibers were collected on electrically grounded aluminum foil placed at a 15-cm vertical distance to the needle of syringe. For comparison, SA/PVA blend nanofibers were prepared by the similar procedure with the same mass concentration and volume ratios ranging from 70/30 to 20/80.

The preparation process of drug-loaded AAD/PVA blend nanofibers can be described as Scheme 1. Briefly, 0.50 g of λ-cyhalothrin and 1.00 g of AAD were dissolved in 50 mL of distilled water at 70 °C, which is higher than the melting point of λ-cyhalothrin (49.2 °C) and vigorously stirred overnight to form the nanocapsule solution. Then, 10.0 wt% PVA solution was prepared by dissolving precise amount of PVA in distilled water and continuously stirred at 80 °C for 5 h [37]. PVA solution was mixed with the nanocapsule solution with the volume ratios of 20/80 of AAD to PVA. Subsequently, the drug-loaded AAD/PVA blend nanofibers were fabricated following the above method. By contrast, the drug-loaded AAD/PVA (50/50) blend nanofibers and the drug-loaded SA/PVA (20/80) blend nanofibers were prepared with the same mass concentration and the same amount of λ-cyhalothrin.

Characterization of blend solutions and as-prepared blend nanofibers

The morphology of the electrospun blend nanofibers was recorded with an S-3000 N scanning electron microscope (SEM, Hitachi, Japan) after gold coating. The fiber diameters were measured from the SEM images with Photoshop 5.0

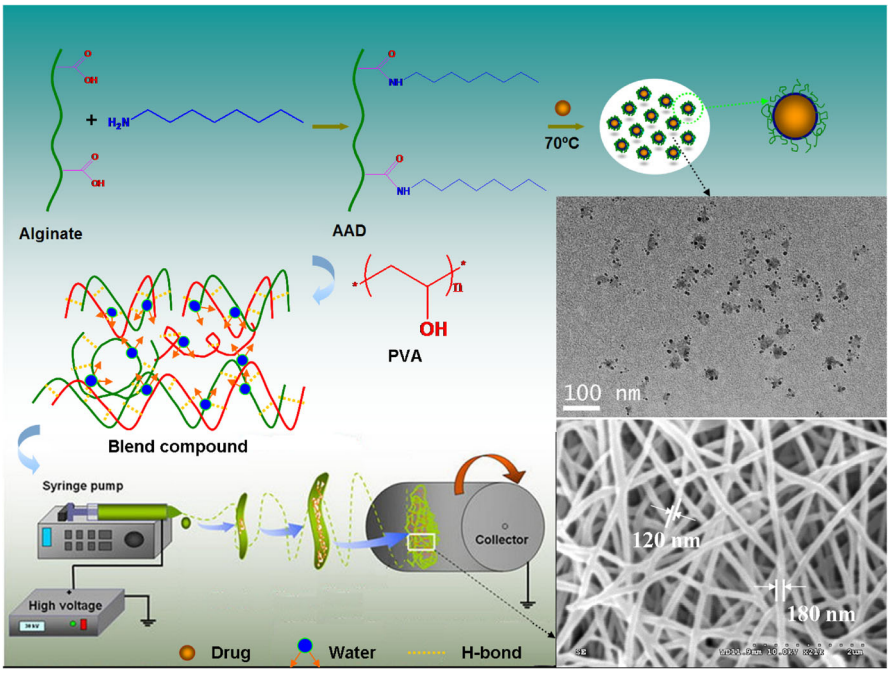

Scheme 1 Schematic diagram of fabrication of drug-loaded blend nanofibers

software. The nanocapsules were observed by a JEM 2100 transmission electron microscope (TEM, Hitachi, Japan) at the acceleration voltage of 200 kV. TEM images of the nanocapsules were obtained by placing a few drops of the nanocapsules solution on a carbon-coated copper grid, and evaporating them prior to observation. The interaction between PVA and AAD was confirmed by the FT-IR spectra using a Tensor 27 Fourier transform infrared spectrometer (Bruker, Germany) and X-ray diffraction (XRD) using a AXS/D8 Advance diffractometer with Cu-kα ($\lambda = 0.154$ nm) (Bruker, Germany). The XRD was operated at 40 kV and 100 mA in a step scan mode. The scanning speed was 0.02°/s. X-ray diffraction measurements were performed over a 2θ range of 3°–60°. The surface tensions of SA/PVA blend solutions and AAD/PVA blend solutions were measured by a JK99C surface tension meter (JK99C, Zhongchen Digital Technology Equipment Co., Ltd., Shanghai, China) at 25 °C. Their conductivities were measured by conductivity meter (DDS-11A, Leici Xinjing Instrument Co., Ltd., Shanghai, China).

Release of λ-cyhalothrin

The controlled release tests were carried out following the method described by our previous work [38]. In detail, 50 mg of λ-cyhalothrin loaded blend nanofibers were enclosed into a dialysis bag (cutoff 3500 M_W), and then the bag was immersed in 400 mL of 50 % aqueous methanol solution in a stoppered conical flask. This system was placed in an environment at a constant temperature of 25 °C. 1 mL of the solution was removed at different time intervals for the determination of λ-cyhalothrin by GC analysis using a HP6890N Gas Chromatography (Agilent, USA). The procedure was performed in triplicate and the same dissolution medium was immediately refilled to the flasks with the volume maintained at 400 mL.

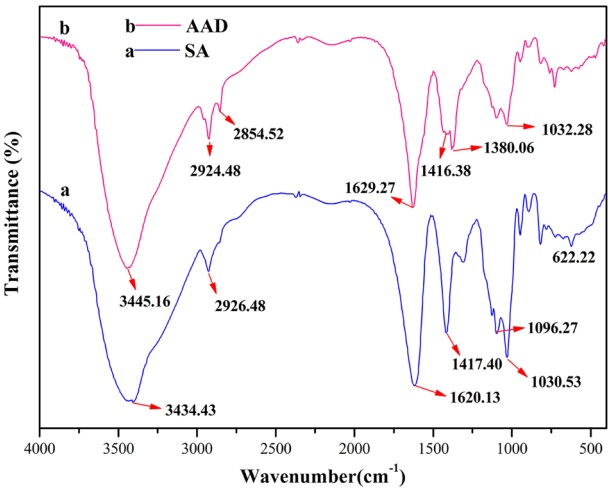

Fig. 1 FT-IR spectra of *a* SA and *b* AAD

Results and discussion

Synthesis and characterization of AAD

The elemental analysis results of SA and AAD were listed as follows: SA: C: 30.17; N: 0.07; H: 5.41; S: 0.175. AAD: C: 33.55; N: 1.30; H: 5.64; S: 0.443, based on which the modification degree of SA was 0.27. The structure of AAD was confirmed by FT-IR (Fig. 1) and ^{1}H NMR (Fig. 2). From the FT-IR spectrum of SA (Fig. 1a), the bands at 1096.27 and 1030.53 cm^{-1} were assigned to C–O–C stretching vibrations [23]. The peak at 2926.48 cm^{-1} was attributed to the stretching vibrations of $–CH_2–$. The characteristic peaks at 1620.13, 622.22 and 1417.40 cm^{-1} were assigned to asymmetric and symmetric stretching vibrations of –COO– [37]. The peak at 1620.13 cm^{-1} in the spectrum of SA (Fig. 1a) shifted to 1629.27 cm^{-1} in that of AAD (Fig. 1b), and the peaks of 2924.48, 2854.52 and 1380.06 cm^{-1} (Fig. 1b) owing to methylene groups of octyl amine and bending vibrations of $–CH_3$ appeared. Furthermore, the peaks of hydroxyl stretching at 3434.43 cm^{-1} in the spectrum of SA (Fig. 1a) shifted to 3445.16 cm^{-1} in that of AAD (Fig. 1b), which was a blue shift effect and the band became sharper after the amidation. The results indicated that the amidation of SA could destroy the original intramolecular

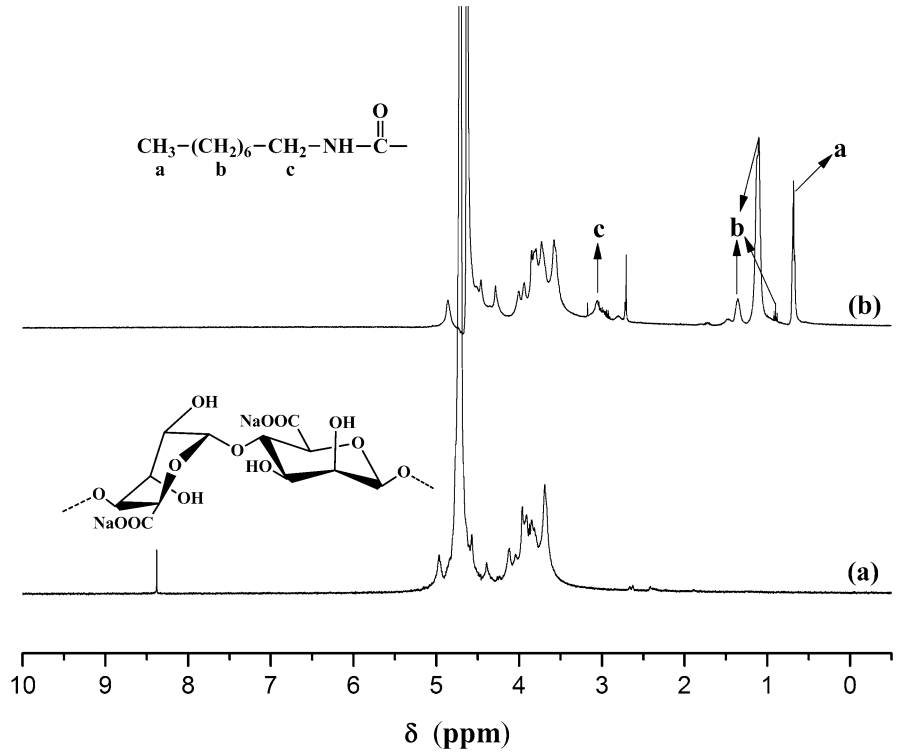

Fig. 2 ^{1}H NMR spectra of *a* SA and *b* AAD

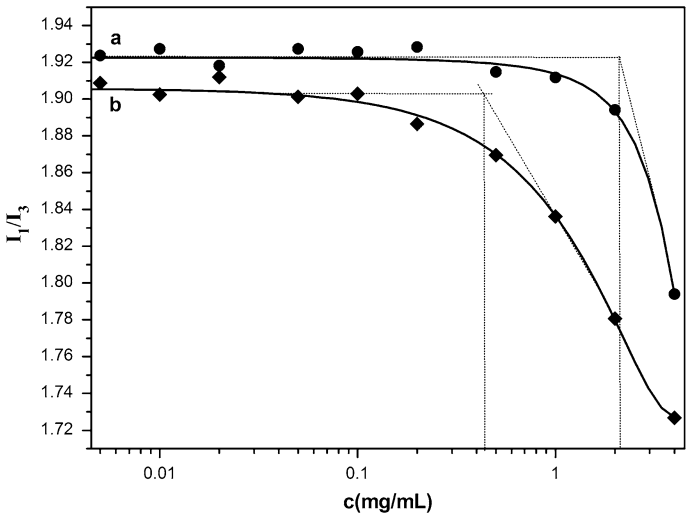

Fig. 3 Plots of pyrene fluorescence intensity I_1/I_3 vs. the concentration of *a* SA and *b* AAD solutions

hydrogen bonding of SA [37], which demonstrated the presence of octyl groups on alginate chains. The successful modification of alginate was further proved by ^{1}H NMR (Fig. 2). Comparing spectrum of SA (Fig. 2a) with that of AAD (Fig. 2b), the proton assignment of the samples was listed as follows: $\delta = 5.0$–3.5 ppm (H of alginate chains), $\delta = 3.5$–0.5 ppm (H of octyl). In detail, the methyl and methylene protons assignment of the octyl was (a) $\delta = 3.0$ ppm (H of –CH_2–NH–), (b) $\delta = 1.4$, 1.0, 0.8 ppm (H of –$(CH_2)_6$–) and (c) $\delta = 0.6$ ppm (H of –CH_3). The amphiphilic property of AAD could be revealed through the fluorescence measurement. And the critical aggregation concentration of AAD was measured according to the ratio value of I_1/I_3, which demonstrated the microenvironmental polarity surrounding pyrene molecules [39]. AAD revealed good amphipathy with low critical aggregation concentration value of 0.43 mg/mL, whereas that of SA was 2.12 mg/mL (as shown in Fig. 3). When the concentration of AAD exceeded 0.43 mg/mL, intermolecular hydrophobic associations can be formed through the hydrophobic interaction between the octyl groups. These associations with hydrophobic drug lead to the formation of nanocapsules [36], which were confirmed by transmission electron microscopy (TEM) with the results showed in Fig. 4. The dried nanocapsules exhibited a nonuniform shape of aggregated structures, resulting from the demulsification and volume shrinkage which occurred when water was evaporated from the as-prepared nanocapsules during the preparation of the TEM samples. The different rates of water loss on the surface eventually led to the irreversible collapse of the nanocapsules' surface. As we can see, the average diameter of the nanocapsules was about 45.4 nm.

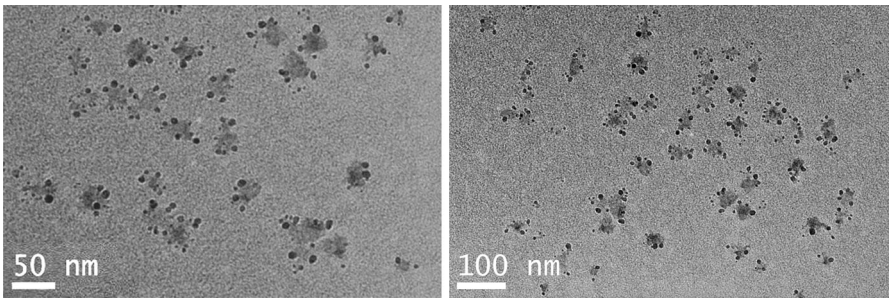

Fig. 4 TEM images of drug-loaded AAD nanocapsules

Electrospinning of AAD/PVA blend solutions

Various parameters, such as electric voltage, tip to collector distance, ratio of polymer component, surface tension and conductivity, could affect the morphology of electrospun nanofibers [37, 40]. The basic parameter of electrospinning is the electrostatic field. The high voltage could make the pendant drop of polymer solution become highly electrified. And then the liquid drop will be deformed into a conical shape known as a Taylor cone under the electrostatic field [41]. When the voltage surpasses a threshold value, the electric force overcomes the surface tension of the droplet and one or multiple charged jets of the solution are ejected from the tip of the droplet. In a fixed tip to collector distance (15 cm) and SA/PVA (30/70), the effect of electrical field on morphological development of blend nanofiber was studied by varying the electrostatic field. As shown in Fig. 5, the nonwoven fabric mats are formed on the aluminum foil under the applied voltage of 10–20 kV. However, the obtained nanofibers exhibit spindle-like morphology in a fixed applied voltage of 10 kV (Fig. 5a). When the applied voltage is up to 15 kV, the uniform nanofibers could be obtained (Fig. 5b, c). So the applied voltage is fixed at 15 kV in our study.

It has been reported that electrospinning of pure alginate from its aqueous solution is difficult to be achieved. The electrospinning of pure AAD solution could not form fabric mats, similar to that of pure SA solution (data not show). To obtain uniform fibers, PVA was introduced into alginate solution. PVA is a kind of

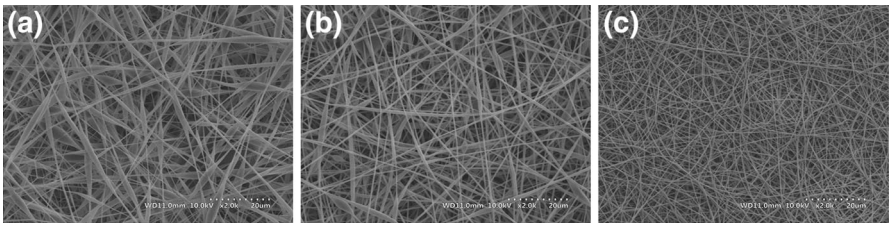

Fig. 5 SEM images of electrospun nanofibers from SA/PVA blend solutions with the volume ratio of 30/70 under the applied voltage of **a** 10 kV, **b** 15 kV and **c** 20 kV

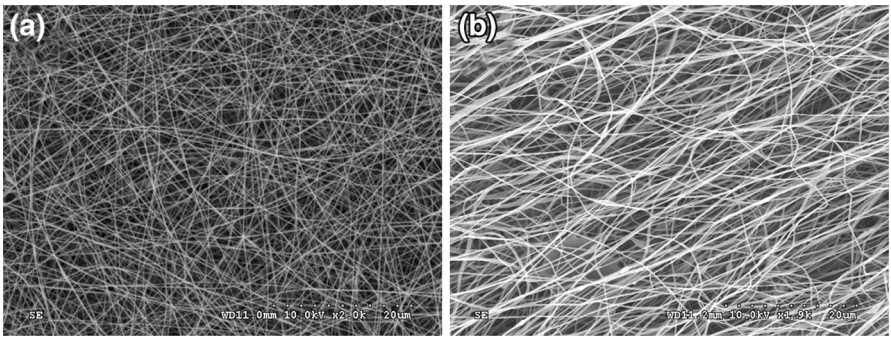

Fig. 6 SEM images of electrospun **a** SA/PVA blend nanofibers and **b** AAD/PVA blend nanofibers with the volume ratio of 20/80 under the applied voltage of 15 kV

miscible hydrophilic synthetic polymer with neutral charge [42]. The hydrogen bonding between PVA and natural SA is responsible for the miscibility and improved spinning properties of the blend solutions [43]. In our study, there was no phase separation phenomenon during the spinning process ascribed to the compatibility of PVA and SA. Figure 6 shows highly uniform nanofibers at 2000× magnification when the volume ratio of AAD or SA to PVA was 20/80, which was consistent with that reported by Islam et al. [37]. The comparison between AAD/PVA blend nanofibers and SA/PVA blend nanofibers revealed that AAD/PVA blend nanofibers presented thick and nonuniform morphology, and they were at the nanoscale with diameters less than 220 nm.

To verify whether the amidation of SA could improve the electrospinnability of alginate solution, 2.0 wt% SA solution was blended with 10.0 wt% PVA solution at various volume ratios in the range of 50/50 to 20/80 in fixed applied voltage of 15 kV. The SEM images of electrospun nanofibers from SA/PVA blend solutions with various volume ratios were shown in Fig. 7. Along with the volume ratios of SA to PVA gradually decreased, SA/PVA blend nanofibers successively exhibited spindle-like beads (50/50), beads on string (40/60), almost bead-free fibers (30/70) and uniform fibers (20/80), which were similar to previous reports [37, 40]. According to Islam et al. [37], the ability of the PVA to influence the electrospinnability of alginate solution requires the presence of PVA chain entanglements via hydrogen bonding interactions between SA and PVA molecules. As increased the PVA content, a higher degree of molecular entanglements was presented to elicit sufficient chain entanglements in the resulting polymer blend solutions that would trigger the fiber formation. When the volume ratio of SA to PVA was 20/80, PVA molecules produced sufficient chain entanglements in the resulting polymer blend solutions to facilitate the fiber formation. The above results indicated that the volume ratio of the polymer solutions played an important role in the formation and morphology of electrospun nanofibers. In contrast to SA/PVA blend solutions, AAD/PVA blend solutions showed more excellent electrospinnability. Indeed, blends of AAD and PVA solutions could be electrospun with few bead defects at relatively high volume ratio of AAD to PVA (50/50), as shown in Fig. 8. As the SA/PVA (70/30) blend solutions could be hardly electrospun in fixed applied

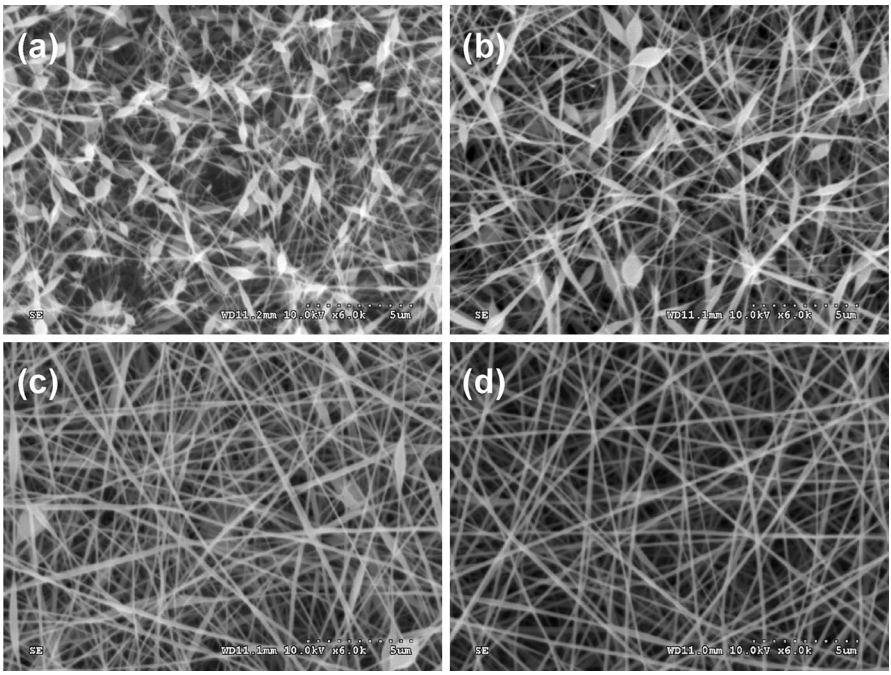

Fig. 7 SEM images of electrospun nanofibers from SA/PVA blend solutions with various volume ratios of 2.0 wt% SA solution to 10.0 wt% PVA solution: **a** 50/50, **b** 40/60, **c** 30/70 and **d** 20/80 under the applied voltage of 15 kV

voltage of 15 kV (data not show), we improved electrostatic voltage. When a high voltage of 20 kV was applied, SA/PVA (70/30) blend nanofibers and AAD/PVA (70/30) blend nanofibers were obtained, as shown in Fig. 9. As seen from the SEM images, AAD/PVA (70/30) blend nanofibers exhibited more uniform and thinner morphology than that of SA/PVA (70/30) blend nanofibers, further indicating that AAD/PVA blend solutions showed more excellent electrospinnability. On the basis of these results, it can be speculated that the amidation of SA could suppress bead defects and facilitate the fiber formation in the process of electrospinning. The rigid and extended worm-like molecular chains of alginate prevent chain entanglement in aqueous solution, which is ascribed to inter- and intra-molecular hydrogen bonding interactions between carboxyl moieties and hydroxyl moieties of alginate molecules [24]. However, the amidation of alginate with octylamine could reduce the alginate's carboxyl moieties and the grafted octyl groups of AAD could form intermolecular hydrophobic associations and make alginate chains flexible through the hydrophobic interactions between octyl groups, which were helpful to weaken and destroy the inter- and intra-molecular hydrogen bonding interactions, consequently improving the spinnability of alginate. Furthermore, it was verified that AAD had the amphiphilic property with the critical aggregation concentration of 0.43 mg/mL. As shown in Table 1, the surface tension and conductivity of SA sharply decreased after the amidation, which could compensate for the increase in

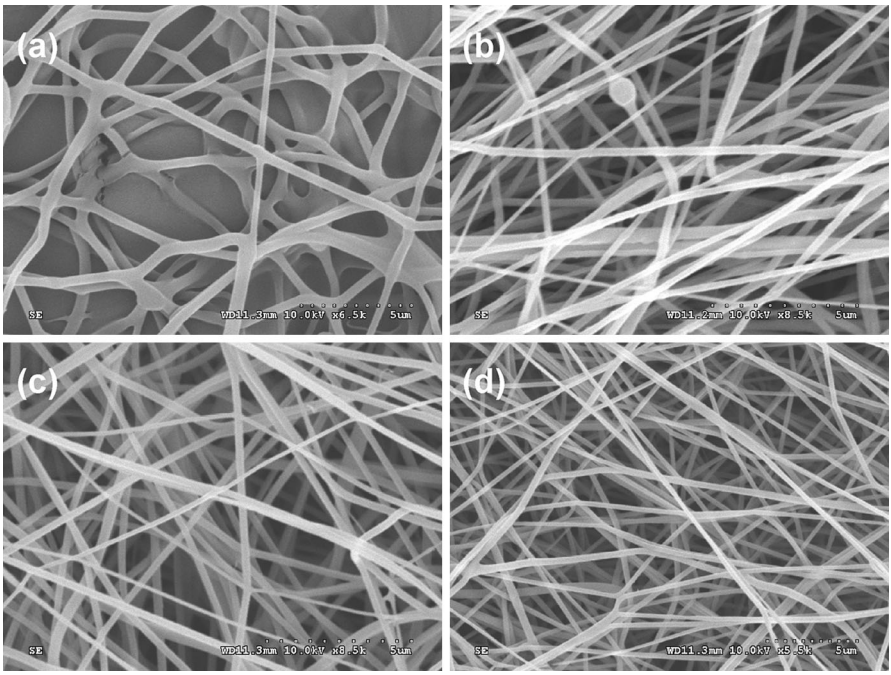

Fig. 8 SEM images of electrospun nanofibers from AAD/PVA blend solutions with various volume ratios of 2.0 wt% AAD solution to 10.0 wt% PVA solution: **a** 50/50, **b** 40/60, **c** 30/70 and **d** 20/80 under the applied voltage of 15 kV

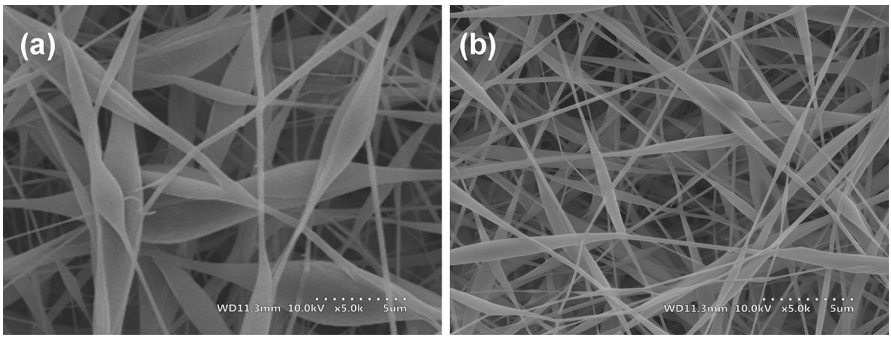

Fig. 9 SEM images of electrospun **a** SA/PVA blend nanofibers and **b** AAD/PVA blend nanofibers with the volume ratio of 70/30 under the applied voltage of 20 kV

alginate concentration and afford the production of higher alginate content fibers. Meanwhile, 2.0 wt% AAD aqueous solution was above its critical aggregation concentration indicating that micelles' formation contributed also to the fiber formation, which was in good accordance with results reported by Yu et al. [44]. As pure AAD solution could not be electrospun, the amidation of SA could not

Table 1 Physical properties of electrospun solutions

Sample[a]	Conductivity (μs cm^{-1})	Surface tension (mN m^{-1})
SA	3854	61.2
AAD	2362	30.6
SA/PVA(20/80)	1177	37.3
AAD/PVA(20/80)	1054	32.7
SA/PVA(50/50)	2636	49.1
AAD/PVA(50/50)	1753	36.9

All data were determined at 25 °C

[a] SA solution was maintained at 2.0 wt%, AAD solution was maintained at 2.0 wt%, PVA solution was maintained at 10.0 wt%

fundamentally alter the spinnability of alginate but appropriately increase the content of alginate in the blend nanofibers.

The physical properties of the electrospun solution were directly related to the ability to form uniform nanofibers [45]. The flexibility and toughness of PVA is good, so it is often used to improve the physical properties through mixing with other materials [37]. The function of PVA maybe is to decrease the conductivity of the solution (as shown in Table 1) and make SA chains become flexible suitable to form chain entanglements. The physical properties of the electrospun solution showed that the amidation of alginate with octylamine led to the decrease in the surface tension and conductivity, which may be attributed to the reduction of alginate's carboxyl moieties grafted by octyl amine. In addition, the lower surface tension was helpful for the electric force to overcome it to form the uniform nanofibers [1]. The generated AAD had many octyl groups and led to self-aggregation formation through the hydrophobic interactions between octyl groups.

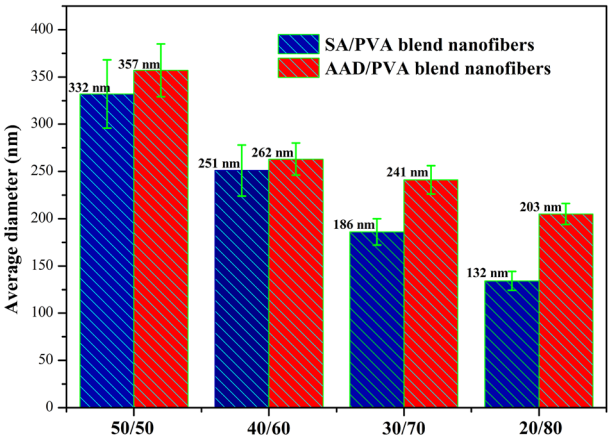

Fig. 10 Average diameters of electrospun SA/PVA blend nanofibers and AAD/PVA blend nanofibers with various volume ratios of 50/50, 40/60, 30/70 and 20/80

The enhanced or improved chain entanglements would improve the fabrication of nanofibers.

In addition to the decrease of surface tension and conductivity, the reduction of alginate's carboxyl moieties during the amidation would weaken the strength of hydrogen bonding formed between AAD and PVA, which could result in the more unsmooth morphology (as shown in Fig. 6) and the higher diameters (as shown in Fig. 10) of AAD/PVA blend nanofibers than SA/PVA blend nanofibers. The interactions between AAD and PVA will be discussed in the following section.

It is found that the SA/PVA blend solutions could be electrospun possibly owing to the hydrogen bonding interactions between SA and PVA molecules [37]. To illustrate the effect of PVA on the formation of AAD/PVA blend nanofibers, FT-IR spectra were used to investigate the interactions between AAD and PVA molecules. Figure 11 shows the FT-IR spectra of AAD, PVA and electrospun AAD/PVA (50/50) blend nanofibers. The frequencies and assignments for AAD spectra are presented as follows: 3445.16 cm^{-1} for –OH stretching vibrations, 2924.48, 2854.52 and 1380.06 cm^{-1} for methylene groups of octyl amine and bending vibrations of $–CH_3$, 1629.27 and 1416.38 cm^{-1} for –COO– group asymmetric and symmetric stretching vibrations, as shown in Fig. 11c [23, 37]. In the spectra of PVA, the bands around 3442.71, 2925.83, 1637.48, 1101.35 and 845.24 cm^{-1} were due to the stretching and bending vibration of –OH, $–CH_2–$, C=O, C–O and C–C group [15, 46], respectively (Fig. 11b). As seen from Fig. 11a, the spectra of AAD/PVA blend nanofibers exhibits the characteristic peaks of AAD and PVA. Obviously, some peaks at 1612.48, 1415.61, 1035.74 and 832.64 cm^{-1} increased while peaks at 1380.06 cm^{-1} disappeared owing to the interactions between AAD and PVA, similar to previous reports [37]. It has been discussed in above section that the original intramolecular hydrogen bonding of SA was destroyed during the amidation. It is worth noting that the bands of hydroxyl stretching in AAD spectra

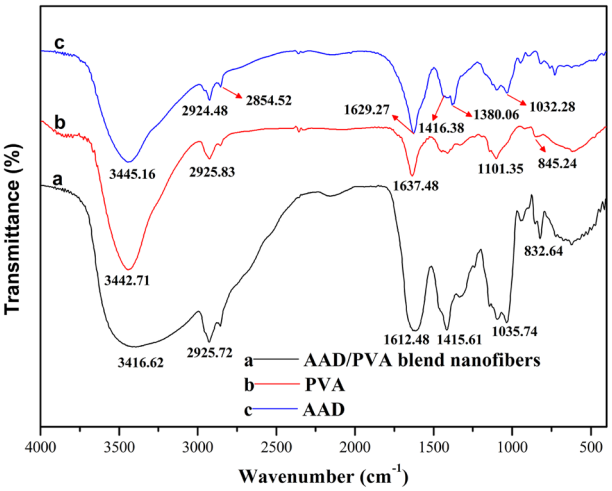

Fig. 11 FT-IR spectra of *a* AAD/PVA (50/50) blend nanofibers, *b* PVA and *c* AAD

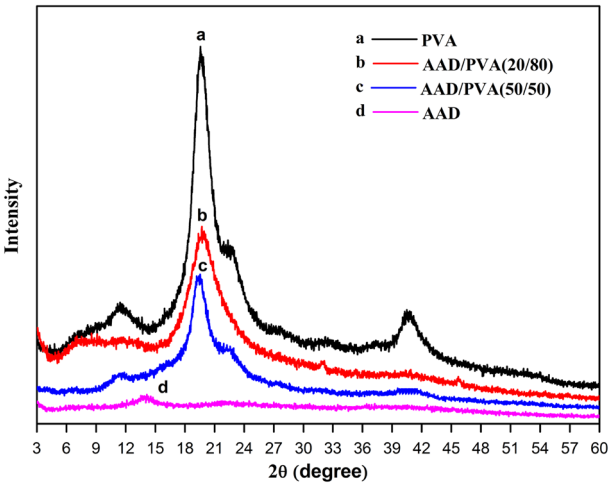

Fig. 12 X-ray diffraction curves of *a* PVA, *b* AAD/PVA (20/80) blend nanofibers, *c* AAD/PVA (50/50) blend nanofibers and *d* AAD

become much broader after blending with PVA with a red shift effect that is hydroxyl stretching at 3445.16 cm^{-1} in the spectrum of AAD (Fig. 11c) shifted to 3416.62 cm^{-1} in the spectrum of AAD/PVA blend nanofibers (Fig. 11a), indicating the formation of the intermolecular hydrogen bonding between AAD and PVA. Therefore, the hydrogen bonding was still the main force between AAD and PVA, as shown in Scheme 1 [37, 46].

The XRD patterns of AAD, PVA and AAD/PVA blend nanofibers are presented in Fig. 12. The weak and broad diffraction peak of AAD at around 13.67° was a typical characteristic peak of the hydrated crystalline structure. The sharp crystalline reflections with a great intensity at 19.52° corresponding to the (110) plane of PVA and a shoulder at 22.75° were primary peaks of the crystalline atactic PVA [15]. There are strong interactions between the polymer chains of PVA, which result from the formation of hydrogen bonding between the hydroxyl groups [47]. However, in the profile of AAD/PVA blend nanofibers, as increased the AAD content, the crystallinity of blend nanofibers decreased, indicating that the crystal structure of PVA was changed after mixing with AAD. The decrease of crystallinity degree of blend nanofibers could probably be ascribed to the formation of hydrogen bonding interaction between AAD and PVA macromolecules, similar to previous reports [37].

Fabrication of the drug-loaded AAD/PVA blend nanofibers

It can be seen from Fig. 13b-1, b-2 that the SEM image of electrospun drug-loaded AAD/PVA blend nanofibers exhibited relatively continuous and uniform nanofibers with the average diameter of 191.72 nm (SD = 13.74 nm). In contrast to Fig. 13b-1, b-2, Fig. 13a-1 and a-2 shows the SEM images of the electrospun drug-loaded

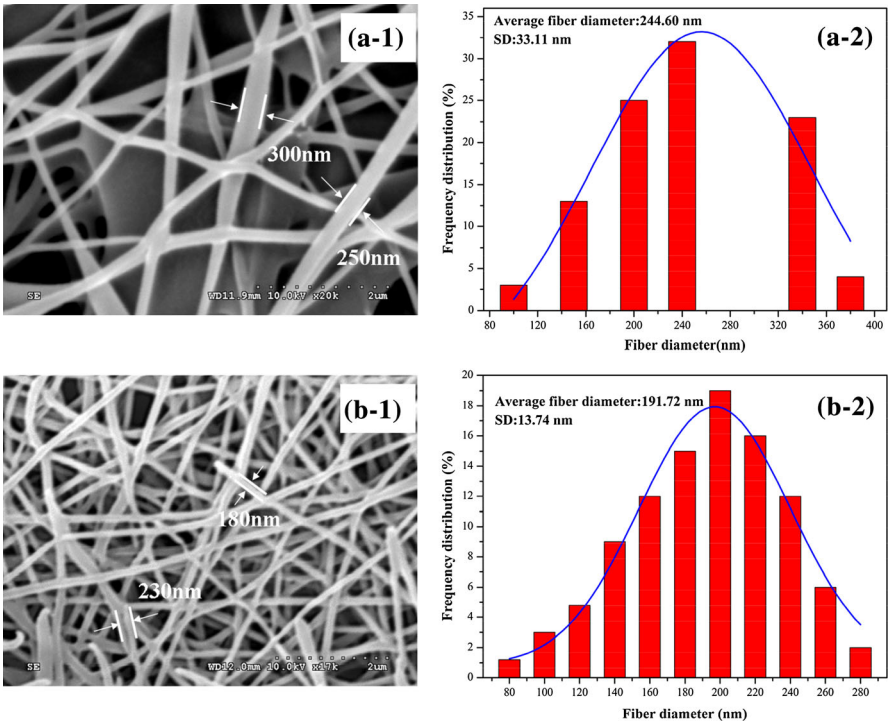

Fig. 13 SEM images of electrospun **a-1** the drug-loaded SA/PVA blend nanofibers and **b-1** the drug-loaded AAD/PVA blend nanofibers with the volume ratio of 20/80; Histograms showing diameter distributions of **a-2** the drug-loaded SA/PVA blend nanofibers and **b-2** the drug-loaded AAD/PVA blend nanofibers

SA/PVA blend nanofibers. The SA/PVA blend nanofibers revealed the nonuniform morphology and not continuous diameter distribution with the average diameter of 244.60 nm (SD = 33.11 nm), which was higher than that of the drug-loaded AAD/PVA blend nanofibers. It is observed that the less amounts of λ-cyhalothrin had great effects on the morphology of the drug-loaded SA/PVA blend nanofibers. Presumably, the reason can be explained by the facts that the SA is too hydrophilic to adjust it with hydrophobic drug, resulting in the incompatibility between SA and λ-cyhalothrin, which may significantly influence the formation of a Taylor cone [48]. On the contrary, the amidation of SA could enhance its affinity to the hydrophobic drug and facilitate the formation of the drug-loaded nanocapsules [21–23], which has little effect on the electrospinnability of AAD/PVA blend solutions.

Release studies

The amidation of SA is needful as it could not only improve the electrospinnability, but also improve the affinity to the hydrophobic drug. The λ-cyhalothrin released from the electrospun AAD/PVA (50/50) blend nanofibers, AAD/PVA (20/80) blend

nanofibers and SA/PVA (20/80) blend nanofibers in 50 % methanol solution at a constant temperature of 25 °C are presented in Fig. 14. The release behavior of the drug-loaded SA/PVA (20/80) blend nanofibers presented a burst release within 5 h, with the release of about 78 % λ-cyhalothrin owing to the water-soluble and biodegradable properties of SA and PVA [15, 49]. The burst release could be effectively inhibited by the amidation of SA. As shown in Fig. 14b, the drug-loaded AAD/PVA (20/80) blend nanofibers exhibited sustained release performance with the slow release of about 76 % λ-cyhalothrin during the initial period of 10 h. The effect of PVA on drug release of different volume ratio of AAD/PVA blend nanofibers was studied by comparing the drug release behavior of AAD/PVA (20/80) blend nanofibers with that of AAD/PVA (50/50) blend nanofibers. As seen from Fig. 14c, AAD/PVA (50/50) blend nanofibers possessing lower PVA content exhibited more sustained release performance than AAD/PVA (20/80) blend nanofibers, which was ascribed to the poor compatibility between PVA and hydrophobic drug. So, the hydrophilic PVA is unfavorable for sustained release of hydrophobic drug. To facilitate the analysis of the effect of the amidation of SA on the release of λ-cyhalothrin, the following model equation was introduced to analyze the release process [50].

$$[M_t/M_\infty = Kt^n]$$

where M_t/M_∞ is the fractional release of drug in time t, K is a constant incorporating structural and geometrical characteristics of the delivery system and n is the diffusion exponent characteristic of the release mechanism. For normal Fickian diffusion, the value of n is 0.5, and for case II diffusion n is 1.0. The values of n intermediate between the above limits indicate non-Fickian transport [50, 51] which occurs when the diffusion and degradation rates are comparable.

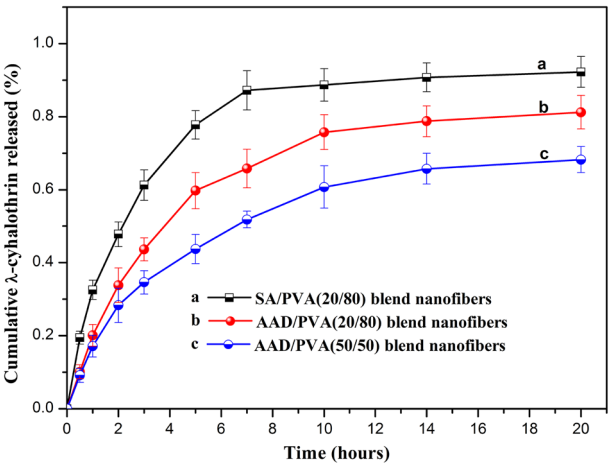

Fig. 14 Release profiles of λ-cyhalothrin from *a* the drug-loaded SA/PVA (20/80) blend nanofibers, *b* the drug-loaded AAD/PVA (20/80) blend nanofibers and *c* the drug-loaded AAD/PVA (50/50) blend nanofibers (*error bars* represent the standard deviation of three replicates)

Table 2 Data fitting results for the release profiles of λ-cyhalothrin

Sample	K (h^{-n})	n	R^2	Diffusion mechanism
SA/PVA (20/80)[a] blend nanofibers	0.3103 ± 0.0006[b]	0.6315 ± 0.0041[c]	0.9956	Non-Fickian
AAD/PVA (20/80) blend nanofibers	0.1868 ± 0.0004	0.7647 ± 0.0053	0.9912	Non-Fickian
AAD/PVA (50/50) blend nanofibers	0.1620 ± 0.0006	0.6456 ± 0.0062	0.9903	Non-Fickian

[a] Value represents the volume ratio of 2.0 wt% SA solution or 2.0 wt% AAD solution to 10.0 wt% PVA solution

[b] Value represents the standard deviation of the constant of K

[c] Value represents the standard deviation of the diffusion exponent of n

The model was applied in data analysis where $M_t/M_\infty < 0.6$. According to the correlation coefficient R^2 as shown in Table 2, the release curves of the electrospun AAD/PVA blend nanofibers and SA/PVA blend nanofibers were fitted well with the model equations. The n values of the electrospun AAD/PVA blend nanofibers and SA/PVA blend nanofibers were between 0.5 and 1.0, which showed that the release of λ-cyhalothrin from the blend nanofibers happened through non-Fickian diffusion. Therefore, the release of pesticides depended on two simultaneously rate processes, i.e., the diffusion of drug molecules from the nanofibers and the degradation of the blend nanofibers [51]. In comparison with the whole release curve of SA/PVA (20/80) blend nanofibers, that of AAD/PVA (20/80) blend nanofibers and AAD/PVA (50/50) blend nanofibers showed a slower and more sustained release process. In addition, AAD/PVA (50/50) blend nanofibers possessing higher AAD content exhibited more sustained release performance than AAD/PVA (20/80) blend nanofibers. The results could be explained by the facts that the amidation of SA could enhance its affinity to the hydrophobic drug and facilitate the formation of the drug-loaded nanocapsules, which was significant for the sustained release of λ-cyhalothrin. Meanwhile, the amidation modification of alginate is widely used in biomedical application and tissue engineering as a result of its biocompatibility and nontoxicity for humans [33, 34]. Thus, the electrospun AAD/PVA blend nanofibers were good candidates for use in biomedical applications due to their drug-loading and sustained release properties. Therefore, the AAD/PVA blend nanofibers will have potential applications as novel hydrophobic drug carrier materials for both pesticides and medicines owing to the good amphipathy of AAD.

Conclusion

Amphiphilic alginate derivative (AAD) was successfully prepared by amide linkage attachment of octylamine onto the carboxylic group of alginate. It is worthwhile to note that the amidation could destroy the original intramolecular hydrogen bonding of SA. The physical properties of electrospun solutions showed that the amidation of

alginate led to the decrease in the surface tension and conductivity, which may be useful to improve spinnability of alginate. The generated AAD with many octyl groups could lead to self-aggregation formation through the hydrophobic interactions between octyl groups, which make alginate chains become flexible and enhance chain entanglements.

Subsequently, AAD/PVA blend nanofibers were successfully fabricated by electrospinning method using 2.0 wt% AAD and 10.0 wt% PVA. The different volume ratios of SA or AAD to PVA played an important role in the formation and morphology of the electrospun blend nanofibers. In contrast to SA/PVA blend solutions, AAD/PVA blend solutions showed more excellent electrospinnability. Furthermore, the diameters of AAD/PVA blend nanofibers for various volume ratios were higher than that of SA/PVA blend nanofibers, respectively, presumably resulting from the decrease of the carboxylic group of AAD after the amidation by octyl amine, weakening the strength of hydrogen bonding formed between AAD and PVA. And the hydrogen bonding was still the main force between AAD and PVA. In addition, the electrospinning of pure AAD solution could not form fabric mat. The uniform fibers could be formed due to the processing benefits of PVA. Consequently, the amidation of SA could not fundamentally alter the spinnability of alginate but appropriately increase the content of alginate in the blend nanofibers. In the release studies, the drug-loaded AAD/PVA blend nanofibers exhibited sustained release performance and could effectively inhibit the burst release, which made the AAD/PVA blend nanofibers have potential applications as novel hydrophobic drug carrier materials for both pesticides and medicines.

Acknowledgments We gratefully thank the financial support form the National Natural Science Foundation of China (21366010), Hainan Province Fund (213010), Key Projects in the National Science & Technology Pillar Program during the Twelfth Five-year Plan Period (2011BAE06B06-07).

References

1. Hu XL, Liu S, Zhou GY, Huang YB, Xie ZG, Jing XB (2014) Electrospinning of polymeric nanofibers for drug delivery applications. J Control Release 185:12–21
2. Shalumon KT, Anulekha KH, Nair SV, Chennazhi KP, Jayakumar R (2011) Sodium alginate/poly (vinyl alcohol)/nano ZnO composite nanofibers for antibacterial wound dressings. Int J Biol Macromol 49:247–254
3. Han XJ, Huang ZM, He CL, Liu L, Wu QS (2006) Coaxial electrospinning of PC (shell)/PU (core) composite nanofibers for textile application. Polym Compos 27:381–387
4. Cui W, Li X, Zhou S, Weng JJ (2007) Investigation on process parameters of electrospinning systems through orthogonal experimental design. Appl Polym Sci 103:3105–3112
5. Li D, Xia Y (2004) Electrospinning of nanofibers: reinventing the whell. Adv Mater 16:1151–1170
6. Dersch R, Steinhart M, Boudrio U, Greiner A, Wendorf JH (2005) Nanoprocessing of polymers: applications in medicine, sensorics, catalysis, photonics. Polym Adv Technol 16:276–282
7. Jayaraman K, Kotaki M, Zhang Y, Mo X, Ramakrishna S (2004) Recent advance in polymer nanofibers. J Nanosci Nanotechnol 4:52–65
8. Neppalli R, Marega C, Marigo A, Bajgai MP, Kim HK, Causin V (2010) Poly(ε-caprolactone) filled with electrospun nylon fibers: a model for a facile composite fabrication. Eur Polym J 46:968–976
9. Huang ZM, Zhang YZ, Kotaki M, Ramakrishna S (2003) A review on polymer nanofibers by electrospinning and their applications in nanocomposites. Compos Sci Technol 63:2223–2253
10. Ding B, Li C, Miyauchi Y, Kuwaki O, Shiratori S (2006) Formation of novel 2D polymer nanowebs. Nanotechnology 17:3685–3691

11. Fang DW, Liu Y, Jiang S, Nie J, Ma GP (2011) Effect of intermolecular interaction on electrospinning of sodium alginate. Carbohydr Polym 85:276–279
12. Bu H, Nguyen GTM, Kjøniksen AL (2006) Effects of the quantity and structure of hydrophobes on the properties of hydrophobically modified alginates in aqueous solutions. Polym Bull 57:563–574
13. Yang JS, Zhao JY, Fang Y (2008) Calorimetric studies of the interaction between sodium alginate and sodium dodecyl sulfate in dilute solutions at different pH values. Carbohydr Res 343:719–725
14. George M, Abraham TE (2006) Polyionic hydrocolloids for the intestinal delivery of protein drugs: alginate and chitosan-a review. J Control Release 114:1–14
15. Hua SB, Ma HZ, Li X, Yang HX, Wang AQ (2010) pH-sensitive sodium alginate/poly(vinyl alcohol) hydrogel beads prepared by combined Ca2+ crosslinking and freeze-thawing cycles for controlled release of diclofenac sodium. Int J Biol Macromol 46:517–523
16. Sangamesh GK, Kumaresh SS, Tejraj MA (2003) Synthesis and characterization of polyacrylamide-grafted chitosan hydrogel microspheres for the controlled release of indomethacin. J Appl Polym Sci 87:1525–1536
17. Silva CM, Ribeiro AJ, Figueiredo M, Ferreira D, Veiga F (2006) Microencapsulation of hemoglobin in chitosan-coated alginate microspheres prepared by emulsification/internal gelation. Aaps J 7:903–913
18. Connick WJ, Bradow JH, Wells W, Steward KK, Van TK (1984) Preparation and evaluation of controlled release formulations of 2,6-dichlorobenzonitrile. J Agric Food Chem 32:1199–1205
19. Pepperman AB, Kuan JW (1993) Slow release formulations of metribuzin based on alginate-kaolin-linseed oil. J Control Release 26:21–30
20. Fernández-Pérez M, Villafranca-Sánchez M, González-Pradas E, Martinez-López F, Flores-Céspedes F (2000) Controlled release of carbofuran from an alginate-bentonite formulation: water release kinetics and soil mobility. J Agric Food Chem 48:938–943
21. Cunha AG, Gandini A (2010) Turning polysaccharides into hydrophobic materials: a critical review. Part 2 hemicelluloses, chitin/chitosan, starch, pectin and alginates. Cellulose 17:1045–1065
22. Yang LQ, Zhang BF, Wen LQ, Liang QY, Zhang LM (2007) Amphiphilic cholesteryl grafted sodium alginate derivative: synthesis and self-assembly in aqueous solution. Carbohydr Polym 68:218–225
23. Yang JS, Ren HB, Xie YJ (2011) Synthesis of amidic alginate derivatives and their application in microencapsulation of λ-cyhalothrin. Biomacromolecules 12:2982–2987
24. Nie HR, He AH, Zheng JF, Xu SS, Li JX, Han CC (2008) Effects of chain conformation and entanglement on the electrospinning of pure alginate. Biomacromolecules 9:1362–1365
25. Bonino CA, Krebs MD, Saquing CD, Jeong SI, Shearer KL, Alsberg E, Khan SA (2011) Electrospinning alginate-based nanofibers: from blends to crosslinked low molecular weight alginate-only systems. Carbohydr Polym 85:111–119
26. Bhattarai N, Li Z, Edmondson D, Zhang M (2006) Alginate-based nanofibrous scaffolds: structural, mechanical, and biological properties. Adv Mater 18:1463–1467
27. Lu JW, Zhu YL, Guo ZX, Hu P, Yu J (2006) Electrospinning of sodium alginate with poly(ethylene oxide). Polymer 47:8026–8031
28. Lee YJ, Shin DS, Kwon OW, Park WH, Choi HG, Lee YR, Han SS, Noh SK, Lyoo WS (2007) Preparation of atactic poly(vinyl alcohol)/sodium alginate blend nanowebs by electrospinning. J Appl Polym Sci 106:1337–1342
29. SmidsrØd O (1970) Solution properties of alginate. Carbohydr Res 13:359–372
30. Mackie W, Perez S, Rizzo R, Taravel F, Vignon M (1983) Aspects of the conformation of polyguluronate in the solid state and in solution. Int J Biol Macromol 5:329–341
31. Barro R, Garcia-Jares C, Llompart M, Bollain MH, Cela R (2006) Rapid and sensitive determination of pyrethroids indoors using active sampling followed by ultrasound-assisted solvent extraction and gas chromatography. J Chromatogr A 1111:1–10
32. Tripathi S, Mehrotra GK, Dutta PK (2009) Physicochemical and bioactivity of cross-linked chitosan-PVA film for food packaging applications. Int J Biol Macromol 45:372–376
33. Vallee F, Muller C, Durand A, Schimchowitsch S, Dellacherie E, Kelche C, Cassel JC, Leonard M (2009) Synthesis and rheological properties of hydrogels based on amphiphilic alginate-amide derivatives. Carbohydr Res 344:223–228
34. Galant C, Kjøniksen AL, Nguyen GTM, Knudsen KD, Nystrom B (2006) Altering associations in aqueous solutions of a hydrophobically modified alginate in the presence of β-cyclodextrin monomers. J Phys Chem B 110:190–195
35. Gomez CG, Chambat G, Heyraud A, Villar M, AuzelyVelty R (2006) Synthesis and characterization of a β-CD-alginate conjugate. Polymer 47:8509–8516

36. Liu CG, Desai KGH, Chen XG, Park HJ (2005) Linolenic acid-modified chitosan for formation of self assembled nanoparticles. J Agric Food Chem 53:437–441
37. Islam MS, Karim MR (2010) Fabrication and characterization of poly (vinyl alcohol)/alginate blend nanofibers by electrospinning method. Colloid Surf A 366:135–140
38. Yan HQ, Chen XQ, Wu TT, Feng YH, Wang CX, Li JC, Lin Q (2014) Mechanochemical modification of kaolin surfaces for immobilization and delivery of pesticides in alginate-chitosan composite beads. Polym Bull 71:2923–2944
39. Nouvel C, Frochot C, Sadtler V, Dubois P, Dellacherie E, Six JL (2004) Polylactide-grafted dextrans: synthesis and properties at interfaces and in solution. Macromolecules 37:4981–4988
40. Li W, Li XY, Chen Y, Li XX, Deng HB, Wang T, Huang R, Fan G (2013) Poly(vinyl alcohol)/sodium alginate/layered silicate based nanofibrous mats for bacterial inhibition. Carbohydr Polym 92:2232–2238
41. Deitzel JM, Kleinmeyer J, Harris D, Beck Tan NC (2001) The effect of processing variables on the morphology of electrospun nanofibers and textiles. Polymer 42:261–272
42. Bhattarai N, Zhang M (2007) Controlled synthesis and structural stability of alginate-based nanofibers. Nanotechnology 18:455601(**10 pp**)
43. He Y, Zhu B, Inoue Y (2004) Hydrogen bonds in polymer blends. Prog Polym Sci 29:1021–1051
44. Talwar S, Krishnan AS, Hinestroza JP, Pourdeyhimi B, Khan SA (2010) Electrospun nanofibers with associative polymer-surfactant systems. Macromolecules 43:7650–7656
45. Nie HR, He AH, Wu WL, Zheng JF, Xu SS, Li JX, Han CC (2009) Effect of poly(ethylene oxide) with different molecular weights on the electrospinnability of sodium alginate. Polymer 50:4926–4934
46. Deng HB, Li XY, Ding B, Du YM, Li GX, Yang JH, Hu XW (2011) Fabrication of polymer/layered silicate intercalated nanofibrous mats and their bacterial inhibition activity. Carbohydr Polym 83:973–978
47. Zhang Y, Huang X, Duan B, Wu L, Li S, Yuan X (2007) Preparation of electrospun chitosan/poly (vinyl alcohol) membranes. Colloid Polym Sci 285:855–863
48. Yarin AL, Koombhongse S, Reneker DH (2001) Taylor cone and jetting from liquid droplets in electrospinning of nanofibers. J Appl Phys 90:4836–4846
49. Zeng J, Xu X, Chen X, Liang Q, Bian X, Yang L, Jing X (2003) Biodegradable electrospun fibers for drug delivery. J Control Release 92:227–231
50. Ritger PL, Peppas NA (1987) A simple equation for description solute release. J Control Release 5:23–36
51. Singh B, Sharma DK, Kumar R, Gupta A (2009) Controlled release of the fungicide thiram from starch–alginate–clay based formulation. Appl Clay Sci 45:76–82